Published in final edited form as:
Spectrochim Acta A Mol Biomol Spectrosc. 2003 September ; 59(11): 2611–2617.

Enhanced photostability of ICG in close proximity to gold colloids

Chris D. Geddes*, **Haishi Cao**, and **Joseph R. Lakowicz**
Department of Biochemistry and Molecular Biology, University of Maryland School of Medicine, Center for Fluorescence Spectroscopy, 725 West Lombard Street, Baltimore, MD 21201, USA

Abstract

Photobleaching of fluorophores frequently limits their detectability or observation time. We examined Indocyanine green (ICG) which is widely used in medical testing and is highly unstable. We showed that spatial localization of ICG near metallic gold colloids resulted in increased photostability. This suggests the use of fluorophore–metal conjugates in situations adversely affected by photobleaching.

Keywords

Fluorescence; Photostability; Indocyanine green; Gold colloids

1. Introduction

Photobleaching or phototransformation of fluorophores is a ubiquitous problem in the applications of fluorescence. Rapid photobleaching occurs for most probes in fluorescent microscopy, where the incident intensities are high and the effective sample volumes are small. Photobleaching is typically observed with the highly useful long-wavelength cyanine dyes due to flexibility around the unsaturated bonds.

Recently, we have been investigating the interactions of metallic multi-metal particles with fluorophores [1–5]. Excited state fluorophores act as oscillating dipoles that interact with free electrons in metals [6–8]. This interaction can result in increased or decreased quantum yields and decreased lifetimes. Sub-wavelength size silver and gold particles display a plasmon absorption, which is responsible for these effects. In previous studies, we used silver island films and colloids that seem to be the optimal metal for enhancing.

In contrast to silver, gold displays absorption at visible wavelengths. As a result, a quenching interaction, presumably due to resonance energy transfer (RET), is frequently the dominant effect so that the fluorescence is quenched. In fact, strong quenching by gold colloids have been used to construct molecular beacons with a high contrast ratio [9]. Furthermore, it is known that quenching effects that shorten the lifetime can result in increased photostability because the fluorophores spend less time in the reactive excited state [10]. Additionally, gold colloids are often used in electron microscopy and are finding increasing use due to their large cross sections for light scattering [11–13] and the potential to shift the plasmon resonance by biochemical affinity interactions [14–16].

Based on these considerations, we examined the effects of colloidal gold on the photostability of Indocyanine green (ICG, Fig. 1). ICG was chosen because of widespread use in medical testing [17–19] and growing use as a contrast agent in optical tomography [20–22]. We

*Corresponding author. Tel./fax: + 1-410-706-3149. E-mail address: chris@cfs.umbi.umd.edu (C.D. Geddes).

speculated that the long wavelength absorption and emission wavelengths of ICG may minimize quenching due to the gold absorption while still increasing the photostability.

2. Experimental materials

ICG, human serum albumin (HSA), $HAuCL_4$ and trisodium citrate dihydrate were obtained from Sigma and used without further purification. Concentrations of ICG and HSA were determined using extinction coefficients of ε (780)=130,000 cm^{-1} and ε (278) nm=37,000 cm^{-1}, respectively.

Glass microscope slides were cleaned by immersion in 30% v/v H_2O_2 and 70% v/v H_2SO_4 for 48 h and then washed in distilled water. The glass slides were coated with amino groups by soaking the slides in a 0.5% v/v solution of 3-aminopropyltrimethoxysilane (APS) for 1 h.

Gold colloids were prepared by the citrate reduction of $HAuCL_4$ [25–27]. Some 68 mg $HAuCL_4$ was dissolved in 200 ml water (1 mM) and brought to the boil with vigorous stirring, followed by the addition of 20 ml (38.8 mM) sodium citrate solution. After a further 10 min simmering, the color of the solution changed from a light yellow to deep-red. The solution was then rapidly cooled. The method produces a stable, deep-red dispersion of gold particles [23–25].

APS coated glass slides were coated with gold colloids by immersing in a gold colloid solution for ≈ 90 h, after which time no further increase in glass slide optical density was observed.

Binding the ICG–HSA to the surfaces, whether glass or gold, was accomplished by soaking the glass and gold colloid coated slides in a 30 μm ICG, 60 μM HSA solution overnight, followed by rinsing with water to remove the unbound material.

For photostability experiments, the glass or colloids surfaces were examined in a sandwich configuration in which two coated surfaces faced inwards towards an ≈ 1 μm thick aqueous sample (Fig. 1). The slides were fully coated with APS, but only half coated with gold colloids.

2.1. Methods

Excitation and observation of the sandwiched samples were made by the front face configuration (Fig. 2). Steady state emission spectra were recorded using a SLM 8000 spectrofluorometer with excitation using a Spectra Physics Tsunami Ti: Sapphire laser in the CW (non-pulsed) mode, 200 mW, 760 nm output, attenuated as required. This enabled the samples to be photobleached as required, i.e. for matching the initial steady state intensities or using the same excitation power.

Time-resolved intensity decays were measured using reverse start-stop time-correlated single-photon counting. Vertically polarized excitation at ≈ 760 nm was obtained using a mode-locked argon-ion pumped, cavity dumped Pyridine 2 dye laser with a 3.77 MHz repetition rate. The instrumental response function, determined using the experimental geometry in Fig. 2, for both gold colloid films and glass slides, was typically < 50 ps fwhm. The emission was collected at the magic angle (54.7°), using a long pass filter (Edmund Scientific), which cut off wavelengths < 780 nm, with an additional 830±10 nm interference filter. Carefully undertaken control experiments with gold colloid-coated surfaces without ICG–HSA showed that all scattered light was alleviated by the filter combination, which was an important consideration given the high scattering cross section of the metal colloids [11–13].

2.2. Data analysis

The intensity decays were analyzed in terms of the multi-exponential model:

$$I(t)=\sum_i \alpha_i \exp(-t/\tau_i) \tag{1}$$

where α_i are the amplitudes and τ_i the decay times, $\Sigma\alpha_i$ =1.0. The fractional contribution of each component to the steady-state intensity is given by:

$$f_i=\frac{\alpha_i\tau_i}{\sum_j \alpha_j\tau_j} \tag{2}$$

The mean lifetime of the excited state is given by:

$$\bar{\tau}=\sum_i f_i\tau_i \tag{3}$$

and the amplitude-weighted lifetime is given by:

$$\langle\tau\rangle=\sum_i \alpha_i\tau_i \tag{4}$$

The values of α_i and τ_i were determined by nonlinear least squares impulse reconvolution with a goodness-of-fit χ_R^2 criterion [26].

3. Results

Gold colloids display a strong visible absorption (Fig. 3, top). Following incubation of the APS-treated slides in a gold colloid suspension, the presence of bound colloids was easily visible from the absorption (Fig. 3, bottom). This absorption is almost exclusively due to the gold colloids, as can be seen from the absorption spectrum of the bound colloids without ICG–HSA. Also, the absorption (795 m) and emission (810 nm) wavelengths of ICG are at longer wavelengths than the gold colloid absorption. Examination of the absorption spectra in Fig. 3 reveals a shift in the plasmon absorption for the surface-bound colloids. At present, we do not know if this shift is due to the proximity of the colloids to each other [27] or due to interaction of ICG with the plasmon absorption [28,29].

ICG binds spontaneously to HSA and HSA binds spontaneously to glass. These interactions provided a convenient method to localize ICG near the gold colloids (Fig. 1). Additionally, ICG binding to HSA probably prevented direct contact of ICG and gold, which may have resulted in complete quenching. We examined the photostability of ICG with continuous illumination (Fig. 4). When the same incident intensity was used, the signal on glass was initially higher than on gold (top). However, the photobleaching on gold was slower. Since one is usually concerned with signal level and since incident power is easily adjusted in many experiments, we attenuated the incident power on gold so that the ICG emission intensity was the same as on glass (Fig. 4, bottom). In this case, the enhanced photostability on gold is dramatic.

We speculated that the increased photostability of ICG on gold was due to a decreased lifetime. Fig. 5 shows the time-dependent decay of ICG. The lifetime of ICG–HSA is reduced ≈ 40% on glass compared to being free in solution. This effect has been seen for other fluorophores

bound to glass [2–4], but we do not yet know the origin of this effect. The lifetime of ICG–HSA is dramatically decreased on the gold colloids (Table 1). The decrease is such that the intensity decay was nearly indistinguishable from the instrument response function of the lamp. These measurements suggest the decreased lifetime of ICG as the origin, at least in part, of the increased photostability near gold colloids.

4. Discussion

What are the potential uses of gold colloid–fluorophore conjugates? One possibility is for retinal angiography where ICG is now used to image the choroidal membrane [30–32]. ICG is rapidly bleached under the intense illumination from a fundus camera. The use of conjugates to gold colloids may result in longer image persistence, as well as less leakage from the vasculature. It is also possible that the scattering signals from the colloids could be used to provide additional imaging information. Similar potential exists for optical tomography. One can also imagine the use of fluorophore–colloid conjugates in microscopy, where the increased photostability would allow for longer observation times.

Acknowledgments

This work was supported by the National Center for Research Resources, RR-08119 and the National Institute of Biomedical Imaging and Bioengineering, EB-00682.

References

1. Lakowicz JR. Radiative decay engineering: biophysical and biomedical applications. Anal Biochem 2001;298:1–24. [PubMed: 11673890]
2. Lakowicz JR, Shen Y, D'Auria S, Malicka J, Fang J, Gryczynski Z, Gryczynski I. Radiative decay engineering 2. Effects of silver island films on fluorescence intensity, lifetimes, and resonance energy transfer. Anal Biochem 2002;301:261–277. [PubMed: 11814297]
3. Gryczynski I, Malicka J, Shen Y, Gryczynski Z, Lakowicz JR. Multiphoton excitation of fluorescence near metallic particles: enhanced and localized excitation. J Phys Chem 2002;106:2191–2195.
4. Lakowicz JR, Shen B, Gryczynski Z, D'Auria S, Gryczynski I. Intrinsic fluorescence from DNA can be enhanced by metallic particles. Biochem Biophys Res Commun 2001;286:875–879. [PubMed: 11527380]
5. Malicka J, Gryczynski I, Kusba J, Shen Y, Lakowicz JR. Effects of metallic silver particles on resonance energy transfer in labeled bovine serum albumin. Biochem Biophys Res Commun 2002;294:886–892. [PubMed: 12061790]
6. Chance RR, Prock A, Silbey R. Molecular fluorescence and energy transfer near interfaces. Adv Chem Phys 1978;37:1–65.
7. Gersten JI, Nitzan A. Accelerated energy transfer between molecules near a solid particle. Chem Phys Lett 1984;104:31–37.
8. Gersten J, Nitzan A. Spectroscopic properties of molecules interacting with small dielectric particles. J Chem Phys 1981;75:1139–1152.
9. Dubertret B, Calame M, Libchaber AJ. Single-mismatch detection using gold-quenched fluorescent oligonucleotides. Nat Biotechnol 2001;19:365–370. [PubMed: 11283596]
10. Jovin, TM.; Arndt–Jovin, DJ. FRET microscopy: digital imaging of fluorescence resonance energy transfer. In: Kohen, E.; Hirschberg, JG.; Ploem, JS., editors. Application in Cell Biology, in Cell Structure and Function by Microscopyfluorometry. Academic Press; London: 1989. p. 99-117.
11. Yguerabide J, Yguerabide EE. Light-scattering submicroscopic particles as highly fluorescent analogs and their use as tracer labels in clinical and biological applications—1. Theory. Anal Biochem 1998;262:137–156. [PubMed: 9750128]
12. Yguerabide J, Yguerabide EE. Light-scattering submicroscopic particles as highly fluorescent analogs and their use as tracer labels in clinical and biological applications—2. Experimental characterization. Anal Biochem 1998;262:157–176. [PubMed: 9750129]

13. Schultz S, Smith DR, Mock JJ, Schultz DA. Single-target molecule detection with nonbleaching multicolor optical immunolabels. PNAS 2000;97(3):996–1001. [PubMed: 10655473]
14. Eck D, Helm CA, Wagner NJ, Vaynberg KA. Plasmon resonance measurements of the adsorption and adsorption kinetics of a biopolymer onto gold nanocolloids. Langmuir 2001;17(4):957–960.
15. Melendez J, Carr R, Bartholomew DU, Kukanskis K, Elkind J, Yee S, Furlong C, Woodbury R. A commercial solution for surface plasmon sensing. Sens Actuat B 1996;35–36:212–216.
16. Salamon Z, Macleod HA, Tollin G. Surface plasmon resonance spectroscopy as a tool for investigating the biochemical and biophysical properties of membrane protein systems. II: Applications to biological systems. Biochim Biophys Acta 1997;1331:131–152. [PubMed: 9325439]
17. Sakka SG, Reinhart K, Wegscheider K, Meier-Hellmann A. Comparison of cardiac output and circulatory blood volumes by transpulmonary thermo-dye dilution and transcutaneous Indocyanine green measurement in critically ill patients. Chest 2002;121(2):559–565. [PubMed: 11834672]
18. Ishihara H, Okawa H, Iwakawa T, Umegaki N, Tsubo T, Matsuki A. Does Indocyanine green accurately measure plasma volume early after cardiac surgery? Anesthes Analges 2002;94(4):781–786.
19. Lanzetta P. ICGA-guided laser photocoagulation of feeder vessels of choroidal neovascular membranes in age-related macular degeneration. Retina J Ret VIT Dis 2001;21(5):563–564.
20. Becker A, Riefke B, Ebert B, Sukowski U, Rinneberg H, Semmier W, Licha K. Macromolecular contrast agents for optical imaging of tumors: comparison of indotricarbocyanine-labeled human serum albumin and transferrin. Photochem Photobiol 2000;72(2):234–241. [PubMed: 10946578]
21. Ntziachristos V, Yodh AG, Schnall M, Chance B. Concurrent MRI and diffuse optical tomography of breast after Indocyanine green enhancement. PNAS 2000;97(6):2767–2772. [PubMed: 10706610]
22. Sevick-Muraca EM, Lopez G, Reynolds JS, Troy TL, Hutchinson CL. Fluorescence and absorption contrast mechanisms for biomedical optical imaging using frequency-domain techniques. Photochem Photobiol 1997;66(1):55–64. [PubMed: 9230705]
23. Lala N, Chittiboyina AG, Chavan SP, Sastry M. Biotinylation of colloidal gold particles using interdigitated bilayers: a UV-visible spectroscopy and TEM study of the biotin-avidin molecular recognition process. Colloids Surf A: Physicochem Eng Asp 2002;205:15–20.
24. Liz-Marzan LM, Giersig M, Mulvaney P. Synthesis of nanosized gold-silica core-shell particles. Langmuir 1996;12:4329–4335.
25. Grabar KC, Freeman RG, Hommer MB, Natan MJ. Preparation and characterization of Au colloid monolayers. Anal Chem 1995;67(4):735–743.
26. Laczko G, Gryczynski I, Gryczynski Z, Wiczk W, Malak H, Lakowicz JR. A 10-Ghz frequency-domain fluorometer. Rev Sci Instrum 1990;61:2331–2337.
27. Storhoff JJ, Elghanian R, Mucic RC, Mirkin CA, Letsinger RL. One-pot colorimetric differentiation of polynucleotides with single base imperfections using gold nanoparticle probes. J Am Chem Soc 1998;120:1959–1964.
28. Garoff S, Weitz DA, Gramila TJ, Hanson CD. Optical absorption resonances of dye-coated silver island films. Opt Letts 1981;6(5):245–247. [PubMed: 19701391]
29. Franzen S, Folmer JCW, Glomm WR, O'Neal R. Optical properties of dye molecules adsorbed on single gold and silver nanoparticles. J Phys Chem 2002;106:6533–6540.
30. Flower RW. Experimental studies of Indocyanine green dye-enhanced photocoagulation of choroidal neovascularization feeder vessels. Am J Opthalmol 2000;129(4):501–512.
31. Schutt F, Fischer J, Kopitz J, Holz FG. Indocyanine green anigography in the presence of subretinal or intraretinal haemorrhages: clinical and experimental investigations. Clin Exp Investigat 2002;30 (2):110–114.
32. Lanzetta P. ICGA-guided laser photocoagulation of feeder vessels of choroidal neovascular membranes in age-related macular degeneration. Retina J Ret VIT Dis 2001;21(5):563–564.

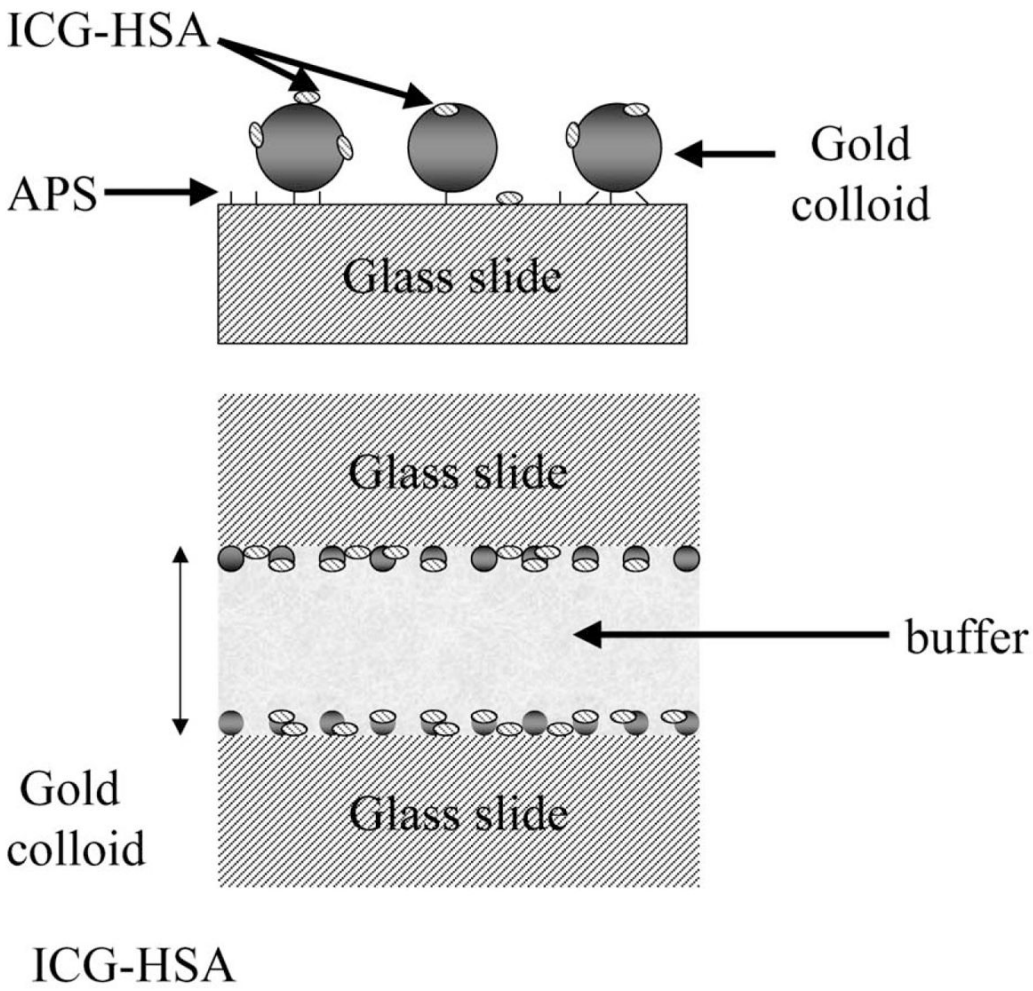

Fig. 1.
Top: chemical structure of ICG; middle: glass surface geometry. APS is used to functionalise the surface of the glass with amine groups which readily bind gold colloids. Bottom: the sample geometry.

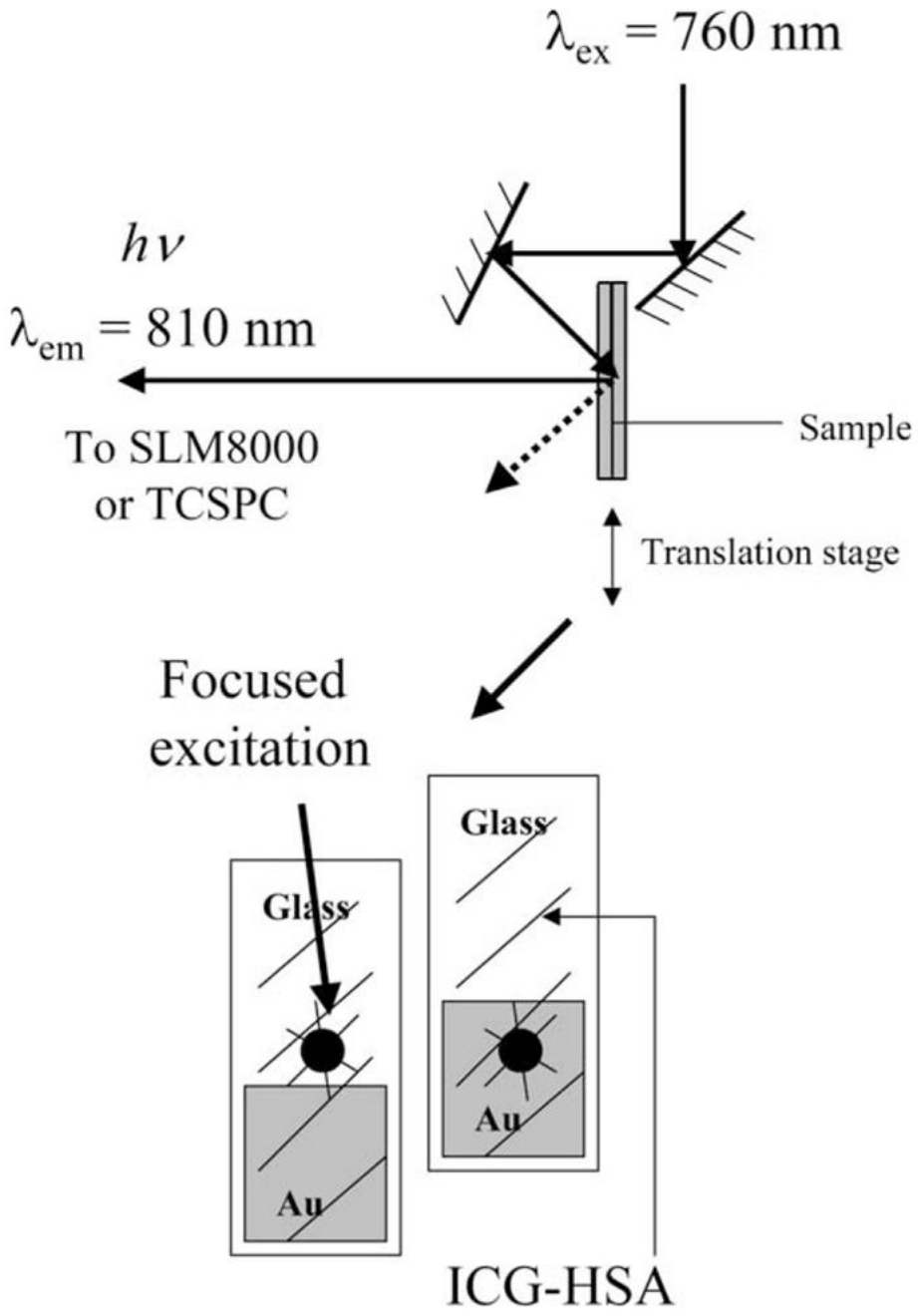

Fig. 2.
Experimental geometry.

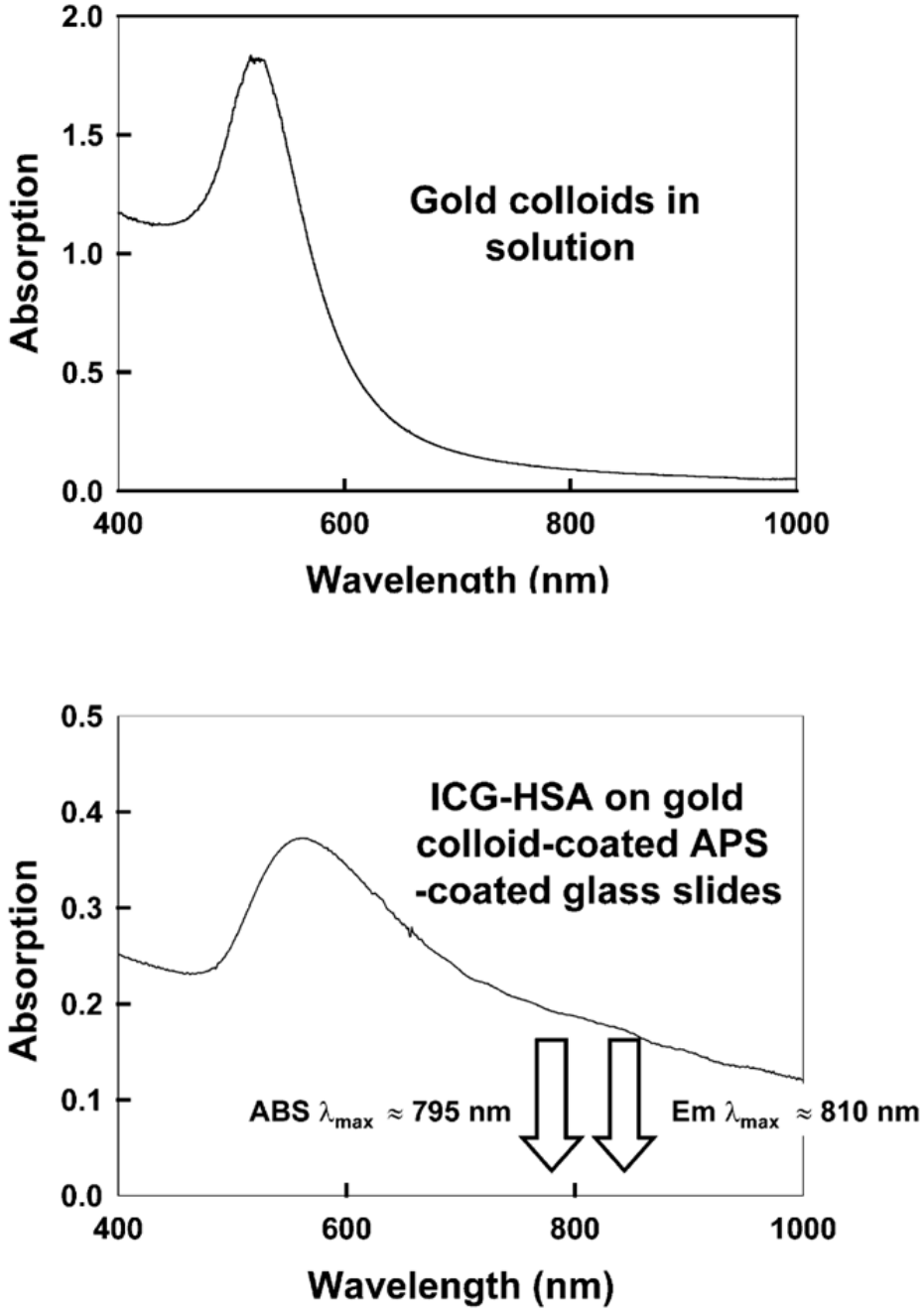

Fig. 3.
Top: absorption spectrum of gold colloids in solution and ICG–HSA-coated APS-coated glass slides.

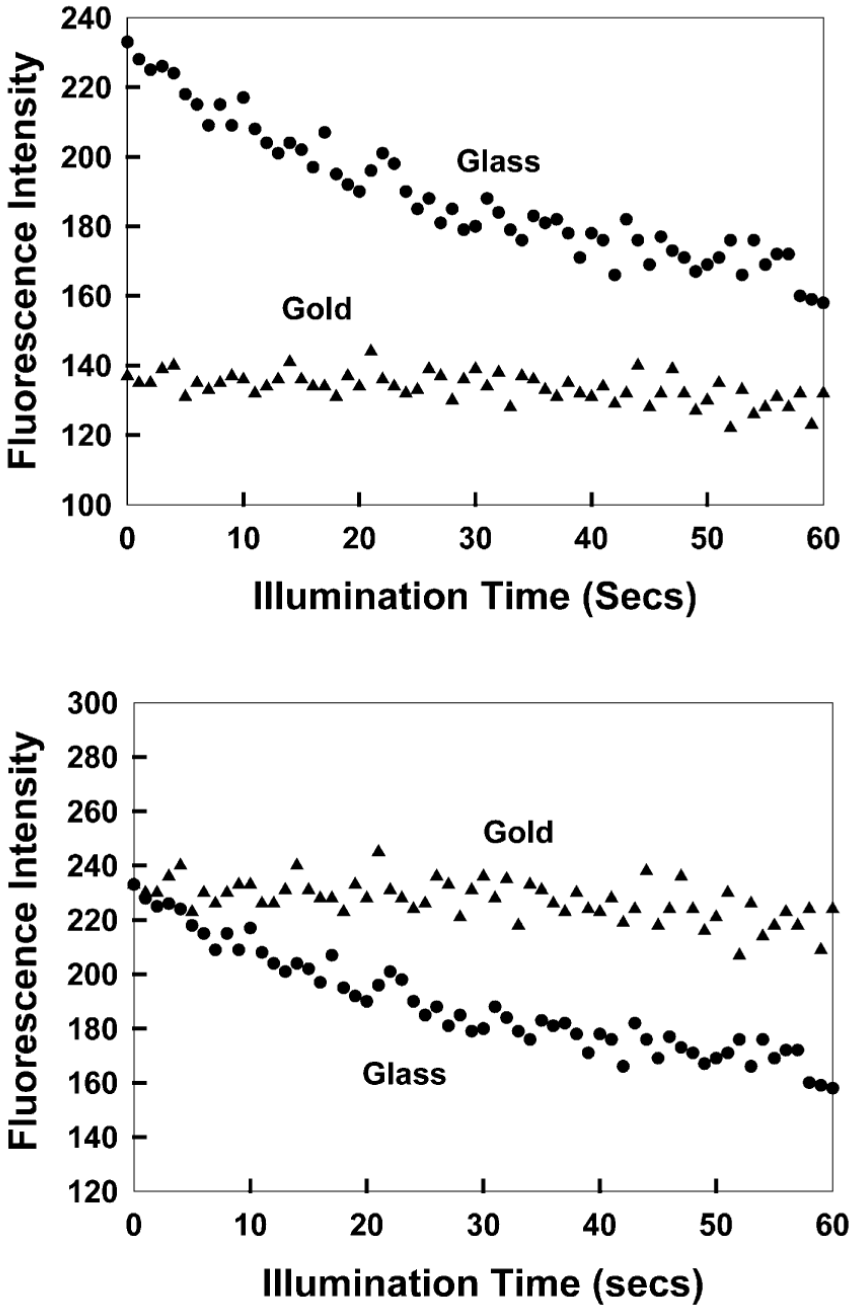

Fig. 4.

Top: photostability of ICG–HSA on glass and gold colloids measured using the same excitation power at 760 nm and (bottom) with power adjusted to give the same initial fluorescence intensities. In all measurements, vertically polarized excitation was used, whilst fluorescence emission was observed at the magic angle, i.e. 54.7°.

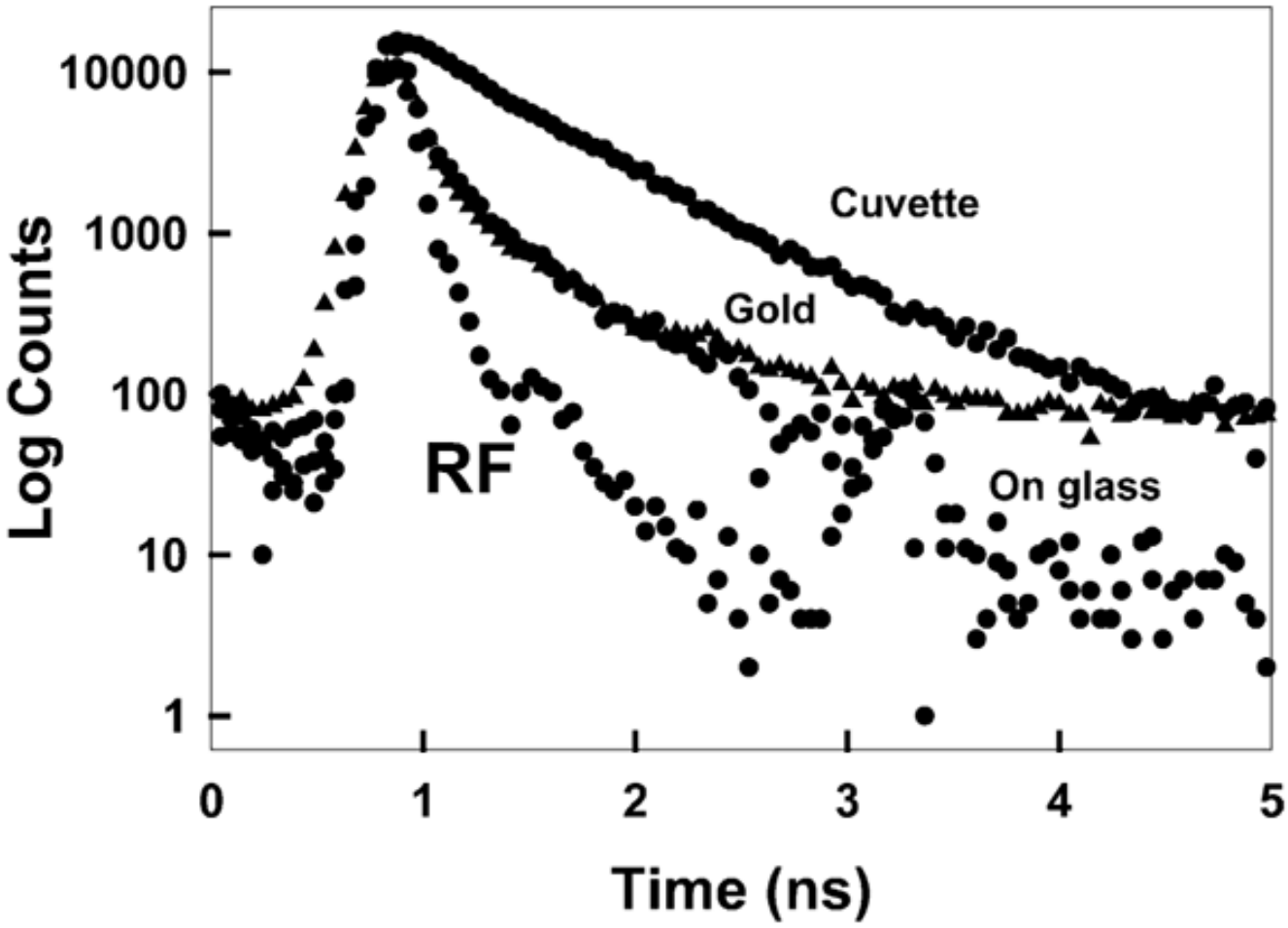

Fig. 5.
Complex intensity decays of ICG–HSA in a cuvette (buffer), on glass slides and gold colloid films (solid triangles). RF, instrumental response function.

Table 1

Analysis of the intensity decay of ICG–HSA measured using the reverse start-stop time-correlated single photon counting technique and the multi-exponential model

Sample	α_i	τ_i(ns)	f_i	$\bar{\tau}$ (ns)	$\langle\tau\rangle$(ns)	χ^2_R
In buffer	0.158	0.190	0.05	–	–	
	0.842	0.615	0.95	0.592	0.548	1.4
On glass	0.683	0.155	0.325	–	–	
	0.317	0.691	0.675	0.517	0.325	1.3
On Au colloids	0.739	0.117	0.359	–	—	
	0.261	0.592	0.641	0.421	0.241	1.8

Spectrochim Acta A Mol Biomol Spectrosc. Author manuscript; available in PMC 2009 September 29.